

Surface plasmon propagation in an elliptical corral

A. Drezet, A. L. Stepanov, H. Ditlbacher, A. Hohenau, B. Steinberger, F. R. Aussenegg, A. Leitner, and J. R. Krenn

*Institut of Physics, Karl-Franzens University Graz,
Universitätsplatz 5 A-8010 Graz, Austria*

(Dated: June 3, 2022)

Abstract

We report the experimental realization of an elliptical Bragg reflector acting as an interferometer for propagating surface plasmon sSPd waves. We investigate SP interferometry in this device using a leakage radiation microscope and we compare our observations with a theoretical model for SP propagation. Strong SP focalization as a function of laser polarization orientation is observed and justified.

Interferometry is at the heart of wave optics. For a long time interferometers were only realizable on the macroscale, however, with the miniaturization of the optical technology, the possibility of realizing microscale interferometers arose. Recent developments towards two-dimensional (2D) optics show that surface plasmons (SPs), which are quasi-2D electromagnetic modes confined at the interface between a dielectric and a metal [1], can interfere and generate fringes [2, 3]. With SPs, unlike in conventional optics, it becomes imaginable to realize highly integrated optical planar devices, allowing one to overcome the classical diffraction limit. The application of SPs to interferometry experiments with micrometer sized devices has been recently exploited for demonstrating a MachZehnder configuration [4], which constituted a first step for the implementation of SP wave optics. In this letter, we extend this precedent work to demonstrating an optical corral for SP waves, by using an elliptical Bragg reflector. In such an elliptical corral, acting as an interferometer, we generate stationary waves by launching a SP in one focal point F_1 , to be focused in the other one F_2 . We describe the observed interferences and SP focalization inside the elliptical corral, and we compare our observations with a simple numerical model.

In order to achieve a significant SP reflectivity and to reduce SP scattering to light we used in Ref. 4 a mirror composed of protrusions on a silver thin film, arranged in parallel lines. To obtain a reflectivity better than 90% we worked in the Bragg regime [5], depending strongly on the SP wavelength λ_{SP} , the separation distance between the protrusions lines, and the incidence angle. However, the Bragg conditions cannot be fulfilled for all directions that appear in a diverging beam. In an elliptical corral, however, the length of all SP paths connecting the two foci $F_{1,2}$ to any point on the mirror equals $2a$, i.e., the long axis length. It is thus straightforward to realize Bragg's condition by using confocal ellipses. Constructive interference between the reflected contributions of the different ellipses will be present only if the variation $\delta(2a)$ of the long axis length between two concentric ellipses is equal to $N\lambda_{SP}$, where N is an integer. As this condition is independent of angle the Bragg resonance is easy to obtain even with divergent SP beams. This property constitutes one of the essential motivations for elaborating an elliptical interferometer. The SP optical elements are obtained by the same electron beam lithography method as described in Ref. 4. The elements, as sketched in Fig. 1(a), are composed of SiO_2 protrusion (160 nm diameter, 80 nm height, center-to-center distance 250 nm), deposited on a glass substrate and covered by a layer of gold of 80 nm thickness. The protrusions are arranged in five confocal ellipses,

all of which share the same two focal points, separated by 30 mm. For a SP wavelength of $\lambda_{SP} \simeq 750$ nm, accessible to a tunable Ti:sapphire laser ($\lambda_0 \simeq 750$ nm)[1], we set δa to 375 nm ($N = 1$). The long half axes of the confocal ellipses measure from $a_{min} = 30$ μm to $a_{max} = 31.5$ μm and the number of protrusions per ellipse varies from $n_{min} = 832$ to $n_{max} = 932$ [compare Fig. 1(a)]. For local SP launch, a single protrusion (160 nm diameter, 80 nm height) is fabricated at the position of F_1 . The measurement of the SP fields is based on a leakage radiation (LR) microscope, sketched in Fig. 1(b). A linearly polarized laser beam is focused with a microscope objective O_1 (50 \times , numerical aperture =0.7) onto the sample plane. By focusing on the single protrusion in F_1 a SP wave is launched[6] in the corral. Due to the presence of the glass substrate the SP is a leaky wave, giving rise to LR along the cone defined by the angle θ_{LR} (which is always larger than the critical angle of total internal reflection), fulfilling the phase matching condition [1, 2, 7]. As the LR intensity is proportional to the SP intensity in any point of the plasmon carrying interface, an immersion objective (O_2 , 63 \times , numerical aperture= 1.25) and a charged-coupled-device (CCD) camera can be used to record leakage radiation images as maps of the SP intensity distribution.

A SP wave generated by a subwavelength protrusion is characterized by a $[\cos(\theta)]^2$ angular intensity distribution, where θ is the azimuthal angle between the polarization axis of the laser and the direction to the observation point. SP reflection at the corral gives rise to a corresponding interference pattern. By rotating the laser polarization with a half wave plate we must then observe modifications of the interferences in the elliptical corral. Figures 2(a) and 2(b) show the interference patterns obtained for two polarization orientations (indicated by the double sided black arrows), while focusing the laser beam onto the single protrusion in F_1 . We see clearly the presence of fringes in the elliptical corral and a strong focalization of the SP beam at F_2 . We note that the grid of white spots in Figs. 2(a) and 2(b) is an artifact from the CCD camera, and that part of the images has been saturated to increase the visibility of the interference pattern. To theoretically model the SP wave we assume at every point on the sample plane the sum of a direct SP Ψ_I launched from F_1 and of a reflected SP Ψ_R coming from the individual protrusions of the mirror. The field is calculated in the first Born approximation [8] and takes into account the $\cos(\theta)e^{ik_{SP}r}/\sqrt{r}$ dependance [2, 6, 9] for the source term (k_{SP} is the complex SP in-plane wave vector and r the distance to the observation point). The response of each individual protrusion is sup-

posed to be proportional to the local SP intensity and is further assumed isotropic with the same radial dependence as Ψ_I . As in Ref. 4 a maximum Bragg mirror reflectivity of 90% is found experimentally, we introduce this value as the only free parameter into the model. The thereby calculated SPs profile in Figs. 2(c) and 2(d) fit the experiment quite well.

In a next step, we decrease the exiting intensity to prevent saturation in the images and thereby allow for quantitative measurement. In Figs. 3 and 4, we compare experiment and theory for different polarization angles θ of the exiting laser beam and, again, we find a good qualitative agreement. From the experimental data we extract the SP intensity in F_2 and plot it in Fig. 5 as a function of the polarization angle θ . Due to the angular dependence of the excitation, Ψ_I must follow a $\cos(\theta)$ law. The same is true for Ψ_R due to interference of the SPs reflected by the protrusions. It is worth mentioning that these interferences come essentially from the angular dependence of the reflectivity of the mirror [10] and not from the complex phase factor $e^{ik_{SP}L}$ which is constant for every SP light path of length $L = 2a$ connecting F_1 and F_2 to any points on the mirror. The total intensity then obeys a $[\cos(\theta)]^2$ law which is perfectly reproduced [11] by the experimental data extracted from Fig. 3 and plotted in Fig. 5.

In summary, we have elaborated an elliptical Bragg reflector acting as a corral for SP waves. SP propagation is observed using a LR microscope which allows quantitative observations and comparison with a theoretical model. By launching a SP wave at F_1 we observe numerous fringes and a strong focalization in F_2 . We can finally realize an angular interferometer by rotating the polarization of the exciting laser beam. In all cases the observations are in qualitative as well as quantitative agreement with our model.

For financial support the Austrian Science Foundation and the European Union, under Project Nos. FP6 NMP4-CT- 2003-505699 and FP6 2002-IST-1-507879, are acknowledged

-
- [1] H. Raether, Surface Plasmons (Springer, Berlin, 1988).
 - [2] B. Hecht, H. Bielefeldt, L. Novotny, Y. Inouye, and D. W. Pohl, Phys. Rev. Lett. 77, 1889 (1996).
 - [3] S. I. Bozhevolnyi and F. A. Pudonin, Phys. Rev. Lett. 78, 2823 (1997).
 - [4] H. Ditlbacher, J. R. Krenn, G. Schider, A. Leitner, and F. R. Aussenegg, Appl. Phys. Lett.

- 81, 1762 (2002).
- [5] M. Born and E. Wolf, Principles of Optics (Cambridge University Press, Cambridge, 1999).
 - [6] H. Ditlbacher, J. R. Krenn, N. Felidj, B. Lamprecht, G. Schider, M. Salemo, A. Leitner, and F. R. Aussenegg, Appl. Phys. Lett. 80, 404 (2002).
 - [7] A. Bouhelier, Th. Huser, H. Tamaru, H.-J. Güntherodt, D. W. Pohl, F. I. Baida, and D. Van Labeke, Phys. Rev. B 63, 155404 (2001).
 - [8] V. Coello, T. Søndergaard, and S. I. Bozhevolnyi, Opt. Commun. 240, 345 (2004).
 - [9] M. Brun, A. Drezet, H. Mariette, N. Chevalier, J. C. Woehl, and S. Huant, Europhys. Lett. 64, 634 (2003).
 - [10] The reflected intensity in F_2 depends on the angular distribution of the protrusions constituting the mirror and on the variation of the damping with the different SP propagation path.
 - [11] The $[\cos(\theta)]^2$ law is in fact valid for every point located on the long ellipse axis. While the intensity at F_2 equals zero theoretically (as can be observed by zooming on this point in the simulation) the LR images in Fig. 3 do not have sufficient spatial resolution to observe this effect. Consequently, the experimental data in Fig. 5 represent the average of the data points around F_2 .

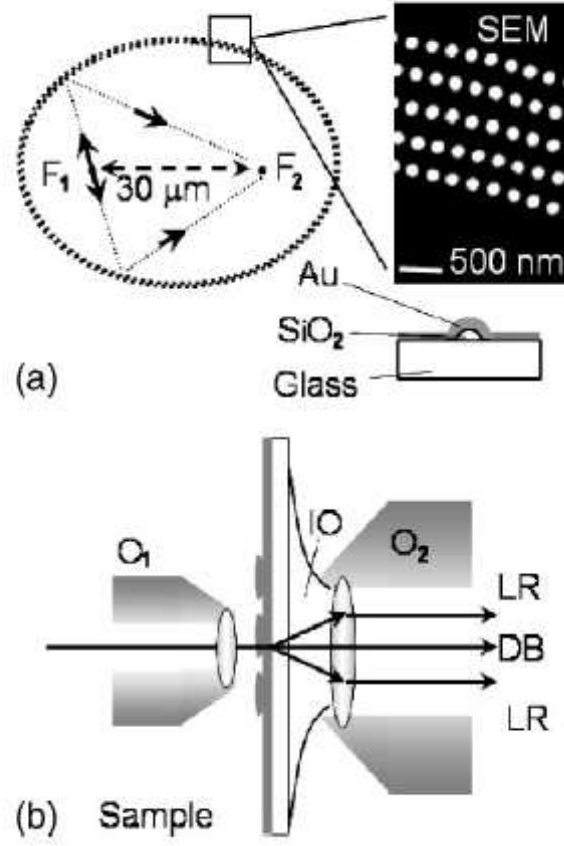


FIG. 1: (a) Outline of the elliptical interferometer together with a scanning electron microscopy image of the mirror structure and a sketch of an individual protrusion. $F_{1,2}$ foci of the ellipse. (b) Sketch of the leakage radiation microscope. $O_{1,2}$ microscope objectives, LR leakage radiation, DB direct beam, IO immersion oil.

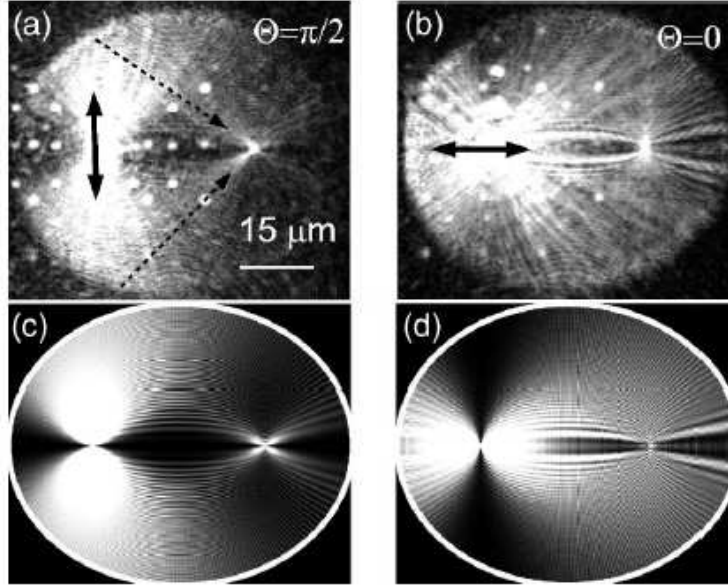


FIG. 2: LR imaging of SP modes propagating in the elliptical corral for (a) vertical ($\theta = \pi/2$) and (b) horizontal polarizations ($\theta = 0$) and $\lambda_0 \simeq 750$ nm. The regular grid of white spots is an artifact from the CCD camera. (c) and (d) The corresponding simulations based on the model.

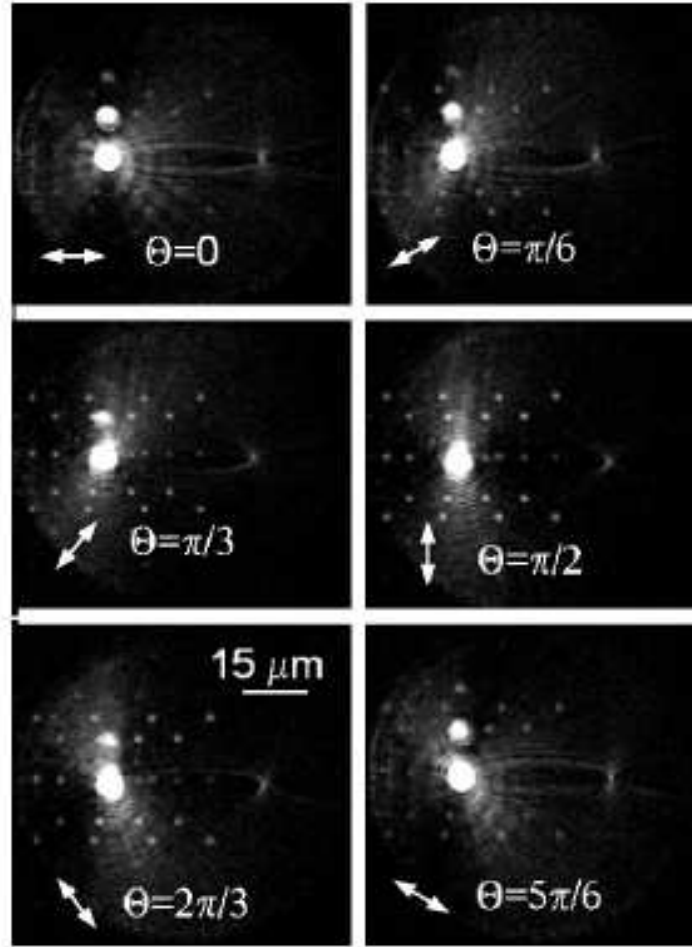


FIG. 3: LR images of SPs wave propagating from F_1 to F_2 for different polarization angles ($\lambda_0 \simeq 750$ nm). The polarization directions are indicated by the double sided white arrows. The regular grid of white spots is an artifact from the CCD camera.

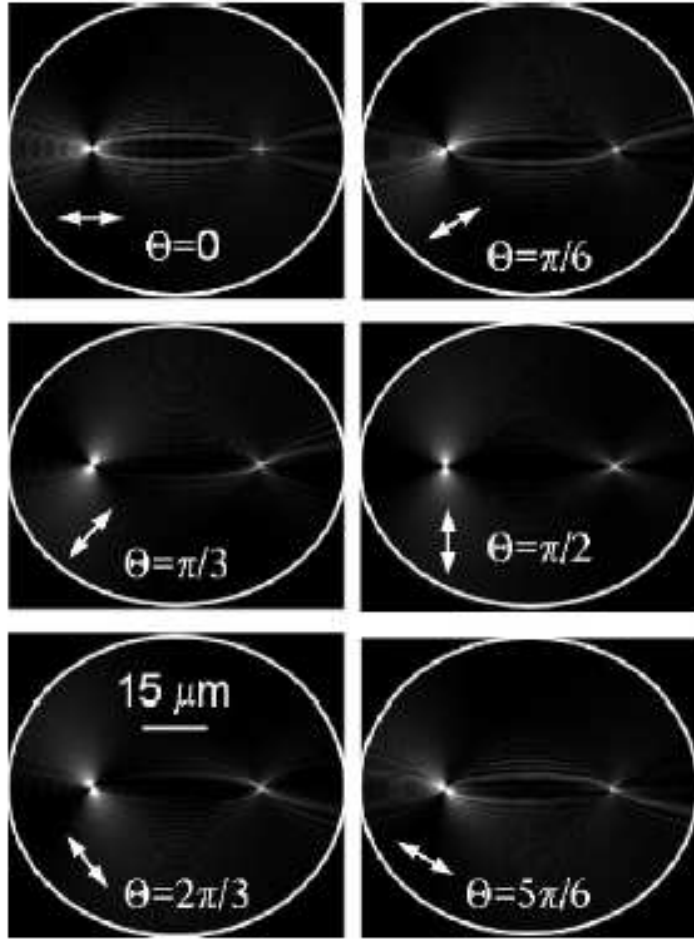


FIG. 4: Simulation of the LR images of Fig. 3. The polarization directions are indicated by the double sided white arrows.

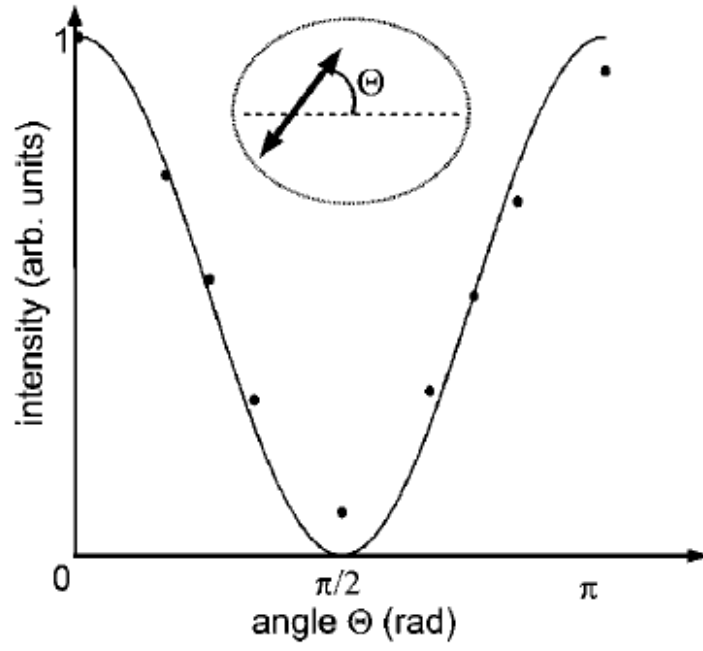


FIG. 5: Experimental data (dots) and theoretical model (solid line) for the dependence of the SP intensity at F_2 on the polarization angle θ .